Journal of Biomechanics 74 (2018) 9–15

Contents lists available at ScienceDirect

Journal of Biomechanics

journal homepage: www.elsevier.com/locate/jbiomech
www.JBiomech.com

Anterior laxity, lateral tibial slope, and *in situ* ACL force differentiate knees exhibiting distinct patterns of motion during a pivoting event: A human cadaveric study

Robert N. Kent III [a,*], Mark J. Amirtharaj [a], Brendan M. Hardy [a], Andrew D. Pearle [b], Thomas L. Wickiewicz [b], Carl W. Imhauser [a]

[a] *Department of Biomechanics, Hospital for Special Surgery, Weill Medical College of Cornell University, New York, NY, United States*
[b] *Department of Orthopedic Surgery, Hospital for Special Surgery, Weill Medical College of Cornell University, New York, NY, United States*

ARTICLE INFO

Article history:
Accepted 1 April 2018

Keywords:
Knee
Instability
Multiplanar torques
Bony geometry
Laxity
ACL
Pivot shift

ABSTRACT

Knee instability following anterior cruciate ligament (ACL) rupture compromises function and increases risk of injury to the cartilage and menisci. To understand the biomechanical function of the ACL, previous studies have primarily reported the *net change* in tibial position in response to multiplanar torques, which generate knee instability. In contrast, we retrospectively analyzed a cohort of 13 consecutively tested cadaveric knees and found distinct *motion patterns*, defined as the motion of the tibia as it translates and rotates from its unloaded, initial position to its loaded, final position. Specifically, ACL-sectioned knees either subluxated anteriorly under valgus torque (VL-subluxating) (5 knees) or under a combination of valgus and internal rotational torques (VL/IR-subluxating) (8 knees), which were applied at 15 and 30° flexion using a robotic manipulator. The purpose of this study was to identify differences between these knees that could be driving the two distinct motion patterns. Therefore, we asked whether parameters of bony geometry and tibiofemoral laxity (known risk factors of non-contact ACL injury) as well as *in situ* ACL force, when it was intact, differentiate knees in these two groups. VL-subluxating knees exhibited greater sagittal slope of the lateral tibia by 3.6 ± 2.4° ($p = 0.003$); less change in anterior laxity after ACL-sectioning during a simulated Lachman test by 3.2 ± 3.2 mm ($p = 0.006$); and, at the peak applied valgus torque (no internal rotation torque), higher posteriorly directed, *in situ* ACL force by 13.4 ± 11.3 N and 12.0 ± 11.6 N at 15° and 30° of flexion, respectively (both $p \leq 0.03$). These results may suggest that subgroups of knees depend more on their ACL to control lateral tibial subluxation in response to uniplanar valgus and multiplanar valgus and internal rotation torques as mediated by anterior laxity and bony morphology.

1. Introduction

Knee instability during pivoting events is characterized by sudden, unexpected subluxation (i.e., partial dislocation) of the tibiofemoral joint, and it is a hallmark feature of the anterior cruciate ligament (ACL)-deficient knee (Galway and MacIntosh, 1980; Houck et al., 2003; Houck and Yack, 2001; Losee, 1983; Noyes et al., 1985; Tamea and Henning, 1981). Instability is associated with poor function, unsatisfactory outcomes, injury to surrounding structures, pain, swelling, and arthritic changes in the knee joint (Conteduca et al., 1991; Jonsson et al., 2004; Noyes et al., 1985). The feeling of instability in the setting of ACL deficiency is reproduced clinically via the pivot shift maneuver; an exam performed by applying a combination of forces and torques while flexing or extending the knee joint (Galway and MacIntosh, 1980; Lane et al., 2008a, 2008b). This maneuver has high specificity for diagnosing ACL rupture and is negatively associated with clinical outcome; therefore, it has become a critical component of diagnosing symptomatic ACL injury (Kocher et al., 2004; Lane et al., 2008a; Leitze et al., 2005; van Eck et al., 2013).

Due to its high clinical relevance, simulation of the pivot shift exam by applying combined, multiplanar valgus and internal rotational torques is commonly used to assess the biomechanical effect of ACL injury and reconstruction (Engebretsen et al., 2012; Fetto and Marshall, 1979; Kanamori et al., 2000b, 2002; Noyes et al., 2015, 2017). Previous biomechanical studies typically quantified the effect of ACL sectioning on knee kinematics by characterizing

* Corresponding author at: Hospital for Special Surgery, 535 E 70th St, New York, NY 10021, United States.

E-mail address: rnkent@umich.edu (R.N. Kent III).

https://doi.org/10.1016/j.jbiomech.2018.04.002
0021-9290/

the net change in primary and coupled motions from an unloaded initial position to a loaded final position (Imhauser et al., 2013; Kanamori et al., 2002; Li et al., 2007; Noyes et al., 2015, 2017; Thein et al., 2016). What is less well characterized is the motion of the tibia as it travels from its unloaded initial position to its loaded final position, which we will refer to as its *motion pattern*. In the absence of muscle forces, knee-to-knee differences in motion patterns must be driven by differences in the articular and ligamentous restraints, as they generate internal reaction forces to resist the externally applied load (Burstein and Wright, 1994). Therefore, assessing the motion patterns of the knee could further characterize the mechanical function of these restraints.

Given that anterior translation of the lateral compartment is the pathological feature of a pivoting event associated with knee instability (Galway and MacIntosh, 1980; Lane et al., 2008a; Losee, 1983), we surmised that it may be important to identify features of bony geometry, joint laxity, and ACL loading that differentiate distinct motion patterns of the lateral compartment. Identifying such features may suggest differences in biomechanical mechanisms driving ACL injury and joint instability (Beynnon et al., 2014; Sturnick et al., 2014; Uhorchak et al., 2003; Vacek et al., 2016). To this end, we asked (1) whether factors that increase risk of noncontact ACL rupture and ACL graft failure including bony geometry (sagittal slope of the medial and lateral compartments, and volume of the medial tibial spine) and tibiofemoral laxity (Beynnon et al., 2014; Magnussen et al., 2016; Sturnick et al., 2014; Uhorchak et al., 2003) differentiate subgroups of knees exhibiting distinct motion patterns; and (2) whether the force carried by the ACL, when it was intact, differed between these subgroups.

2. Methods

2.1. Specimen preparation

Under Institutional Review Board approval, 13 fresh-frozen human cadaveric knees were acquired for testing (mean age: 45 ± 11 years; range: 20–62 years; 8 male). Specimens were stored at −20 °C and thawed for 24 h before undergoing computed tomography (CT) scans (Biograph mCT; Siemens, Munich, Germany) with 0.6 mm slice thickness and $0.5 \times 0.5\ mm^2$ in-plane pixel dimensions (settings: 140 kV and 140 mA). After imaging, all soft tissues were removed from the knee specimens save for the ligaments, capsular tissues, and popliteal muscle-tendon complex (Imhauser et al., 2013). After the fibula was fixed to the proximal tibia with a transverse screw and transected just distal to the screw, the tibia and femur were potted in bonding cement (Bondo, 3 M, St Paul, MN, USA). In addition to the CT data, medial parapatellar arthrotomies, physical examinations, and medical histories were used to confirm that each specimen was free of osseous abnormalities, damage to the soft tissues, malalignment, and prior surgery.

2.2. Robotic testing

Potted specimens were mounted at full extension to a six degrees-of-freedom, serial robot (ZX165U; Kawasaki Robotics, Wixom, MI, USA) with an absolute position accuracy of ±0.3 mm (Kawasaki Robotics, 1999). Custom fixtures rigidly attached the femur to the ground and the tibia to the end effector of the robot. A universal force-moment sensor (Theta; ATI, Apex, NC, USA) (resolution: Fx = Fy = 0.13 N, Fz = 0.25 N, Tx = Ty = Tz = 0.008 Nm; limits: Fx = Fy = 1500 N, Fz = 3750 N, Tx = Ty = Tz = 240 Nm) connected the tibial fixture to the robot's end effector. Specimens were covered in saline-soaked gauze throughout testing to maintain hydration of the cadaveric tissues (Viidik, 1973).

Tibial kinematics and applied loads were described by adapting the specifications of Grood and Suntay (Grood and Suntay, 1983; Imhauser et al., 2013; McCarthy et al., 2013), with anatomical axes oriented in the anterior-posterior (AP), medial-lateral (ML), and proximal-distal (PD) directions. Additionally, anterior translation of the lateral compartment was tracked by projecting the fibular insertion of the LCL onto the AP axis (Bedi et al., 2010; Lane et al., 2008b). Anterior translation of the lateral compartment of the tibia is the pathological feature of pivoting events (Galway and MacIntosh, 1980; Lane et al., 2008a; Losee, 1983); therefore, it is a clinically relevant measure of tibial subluxation.

With the anatomical directions defined, the robot passively flexed the knee from full extension to 90° in 1° increments. At each step in the flexion path, the robot maintained a compressive force of 10 N while minimizing forces and torques in the remaining five directions to within 5 N and 0.4 Nm using a previously described, stiffness-based algorithm (MATLAB; Mathworks, Natick, MA, USA) (Imhauser et al., 2013; Prisk et al., 2010). Next, each knee was set to the respective posterior and external rotational extremes of their anteroposterior and internal-external rotational neutral zones (Tochigi et al., 2011) to define a consistent initial position and orientation. Finally, specimens were preconditioned by applying 134 N of anterior force at 30° of flexion and a combination of valgus (8 Nm) and internal rotation (4 Nm) torques at 15° of flexion and then repeating the resulting kinematics for ten cycles (Imhauser et al., 2013).

At 15° and 30° of flexion, the robot applied multiplanar valgus and internal rotational torques with the ACL intact and sectioned to simulate a pivoting event. These flexion angles are within a range where clinical and functional pivoting events occur (Galway and MacIntosh, 1980; Lane et al., 2008a; Losee, 1983). In particular, the robot incrementally increased the applied valgus torque as follows: 0, 0.8, 2.0, 4.0, 6.0, 7.0, and 8.0 Nm. Then, while holding the valgus torque at a constant 8.0 Nm, the robot increased internal rotation torque in the following increments: 0, 0.4, 0.8, 1.2, 2.0, 3.0, and 4.0 Nm (Noyes et al., 2015; Rasmussen et al., 2016; Schon et al., 2016). The tibia was free to move in all directions save for flexion-extension. To assess the precision of our kinematic measurements at each increment of applied load, in one specimen, the path of motion was determined five independent times. PD, ML, and AP translations had a precision $\leq$±0.2, ±0.2, ±0.5 mm; internal-external, and varus-valgus rotation measurements had a precision $\leq$±1.2° and ±0.2° (flexion was fixed) (Appendix I).

This study is based on the observation that, in response to multiplanar torques, ACL-deficient specimens exhibited two distinct motion patterns: anterior subluxation of the lateral tibia under <5 Nm of isolated valgus torque (i.e., VL-subluxating), or under combined valgus and internal rotation torques (i.e., VL/IR-subluxating) (Fig. 1). To objectively group specimens with distinct motion patterns, a partitioning around medoids algorithm, in which groupings with minimal variance are identified, was used (Kaufman and Rousseeuw, 1987). Specifically, the applied load at which the lateral tibia subluxated 10 mm anteriorly in each ACL-sectioned knee was determined by linear interpolation between adjacent load steps; this amount of lateral tibial subluxation is clinically meaningful because it corresponds to an increase in at least one clinical grade of the pivot shift exam (Bedi et al., 2010). Each knee was then clustered into one of the two groups based on the applied loads at which 10 mm of subluxation occurred (Fig. 1). A sensitivity analysis confirmed that this method was insensitive to the choice of subluxation threshold; thresholds ranging from 4 to 15 mm yielded the same groups at both flexion angles. The two distinct motion patterns were likely not caused by the torque convergence tolerance of 0.4 Nm for our robot test

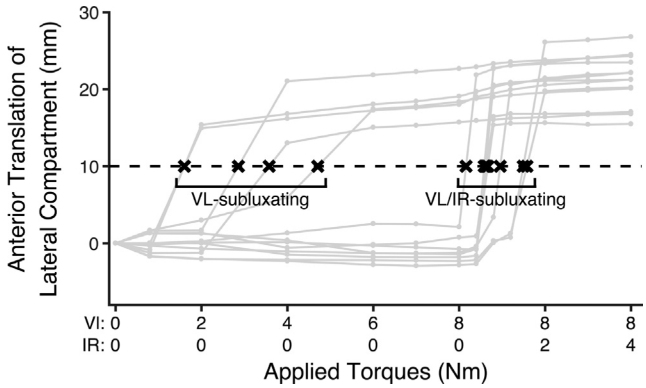

Fig. 1. Demonstration of the partitioning around medoids method used to separate specimens into VL (valgus)- and VL/IR (valgus + internal rotation)-subluxating groups. Grey lines indicate the motion pattern of each knee; specifically, anterior translation of the lateral tibia, in millimeters, as a function of the applied valgus (VL) and internal rotation (IR) torques, in newton-meters (Nm), at 15° of flexion is shown in grey for each individual, ACL-deficient specimen. The applied torques at which the lateral tibia of each knee translated 10 mm anteriorly were identified (black X's) and then used to objectively differentiate VL- and VL/IR-subluxating knees.

algorithms because this tolerance was at least 5 times smaller than the difference between the highest valgus torque at which a VL-subluxating specimen cleared the 10 mm threshold and the lowest valgus torque at which a VL/IR-subluxating specimen cleared this threshold (Fig. 1); these differences were 3.5 Nm and 2.1 Nm at 15° and 30° of flexion, respectively.

2.3. In situ ACL forces

To determine whether the ACL functioned differently in knees with the two distinct motion patterns, *in situ* ACL force was measured via superposition in the ACL-intact knee (Fujie et al., 1995; Woo et al., 1998). Specifically, the valgus and internal rotation torques were applied to the ACL-intact knee, and the kinematics in response to each load increment were measured. This kinematic path was then repeated with the same displacement rate immediately before and after sectioning the ACL. ACL force was then calculated as the vector difference in force measured before and after the ACL was sectioned. Superposition yielded components of the forces imparted on the tibia by the ACL in the AP, ML, and PD directions at each step of the applied multiplanar torque. *In* situ ACL forces were compared between the two groups at the peak applied valgus torque because, at this load step, the lateral compartment of VL-subluxating knees had already subluxated, while the lateral compartment of VL/IR-subluxating knees had not (Fig. 2). At this load increment, proximal, lateral, posterior, and resultant ACL forces had a precision of ±1.6, ±0.5, ±0.5, and ±1.7 N, based on five independently determined kinematic trajectories on a single knee (see Appendix I).

2.4. Laxity assessment

ACL-deficient, uniplanar laxities in both the anterior (simulated Lachman test) and internal rotational directions were independently assessed. Moreover, given that it is a known risk factor for ACL graft rupture (Magnussen et al., 2016), the increase in anterior laxity resulting from ACL sectioning was also determined (see Appendix II). For the simulated Lachman test, we measured the anterior translation of a point in the center of the tibia located at the bisection of the medial and lateral femoral epicondyles; internal rotation was described about the long axis of the tibia (Imhauser et al., 2013; McCarthy et al., 2013).

2.5. Characterization of tibial geometry

Bony geometries of each tibia were obtained from 3D reconstructions of the axial CT scans. Then, using objective algorithms, two aspects of the bony tibial anatomy, namely the volume of the anteromedial tibial spine (also known as the tibial eminence) and the slope of the lateral tibial plateau in the sagittal plane, were calculated because they are risk factors of non-contact ACL rupture (Adams et al., 2018; Beynnon et al., 2014; Sturnick et al., 2014) (see Appendix III). Additionally, the slope of the medial tibial plateau in the sagittal plane was calculated as a control. In both compartments, positive values indicated posterior slopes.

2.6. Statistical analysis

Bony geometric parameters, uniplanar laxities, and *in situ* ACL forces during the simulated pivot were compared between the VL- and VL/IR-subluxating knees using Mann-Whitney U tests ($p < 0.05$). Kolmogorov-Smirnov tests confirmed that each outcome measure was normally distributed ($p < 0.05$), but non-parametric statistical analyses were used due to the small sample size.

3. Results

In the ACL-sectioned condition, the lateral compartment translated anteriorly in all 13 knees, respectively averaging 19.6 ± 3.6 mm and 20.4 ± 4.9 mm of anterior translation at 15° and 30° of flexion between the unloaded, neutral position and the peak applied valgus and internal rotation torques. When assessing our

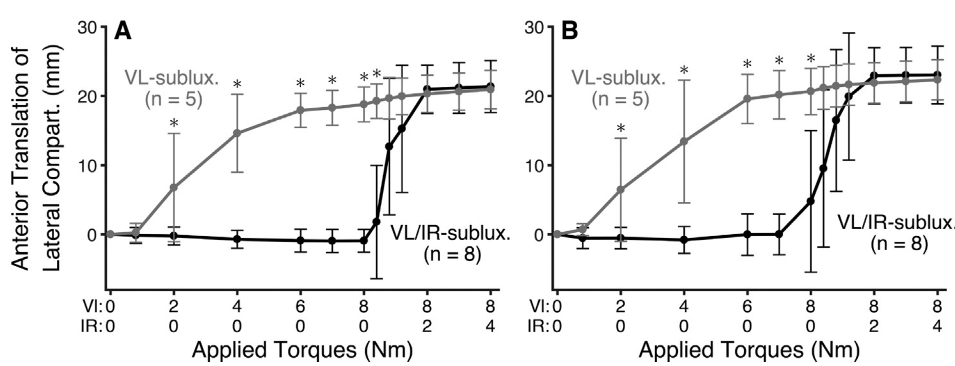

Fig. 2. Anterior translation of lateral tibia with the ACL sectioned for VL (valgus)- and VL/IR (valgus + internal rotation)-subluxating knees in response to the applied valgus and internal rotation torques at (A) 15° and (B) 30° of flexion. Gray lines represent VL-subluxating knees, while black lines represent VL/IR-subluxating knees (mean ± standard deviation). n = sample size. * indicates $p < 0.05$ in anterior translation of the lateral compartment between VL- and VL/IR-subluxating knees.

two subgroups of knees, at both 15° and 30°of flexion (Fig. 2), the same 5 of the 13 ACL-sectioned knees were VL-subluxating, and the remaining 8 knees were VL/IR-subluxating. VL-subluxating knees exhibited greater anterior translation of the lateral compartment from 2.0 and 0.0 Nm of VL and IR torque to 8.0 and 0.4 Nm of VL and IR torque at 15° of flexion compared to VL/IR-subluxating knees. At 30° of flexion, this difference occurred from 2.0 and 0.0 Nm of VL and IR torque to 8.0 and 0.0 Nm of VL and IR torque (all $p < 0.05$). At the peak applied valgus and internal rotation torques, the magnitude of anterior translation of the lateral compartment differed by <0.7 mm at both flexion angles between VL- and VL/IR-subluxating knees (both $p > 0.7$). Tibial kinematics in varus/-valgus and internal/external rotations are included in Appendix IV.

The sagittal slope of the lateral tibial plateau was 3.6 ± 2.4° greater in VL-subluxating knees compared to VL/IR-subluxating knees ($p = 0.003$), while the sagittal slope of the medial tibial plateau showed no difference between these groups ($p = 0.833$) (Table 1). Additionally, the volume of the anteromedial tibial spine was not different between VL- and VL/IR-subluxating knees ($p = 0.724$).

Anterior laxity of the ACL-sectioned knee as assessed by a simulated Lachman was 3.7 ± 2.9 mm ($p = 0.006$) less in VL-subluxating knees compared to VL/IR-subluxating knees (Table 2). Moreover, the increase in anterior laxity caused by ACL sectioning was 3.2 ± 3.2 mm ($p = 0.03$) less in VL-subluxating knees compared to VL/IR-subluxating knees (Table 2). In contrast, statistical differences in internal rotational laxity of the ACL-sectioned knee were not detected between these groups at 15° and 30° of flexion ($p \geq 0.065$) (Table 2).

With the ACL intact, at the peak applied valgus torque (with no applied internal rotational torque) the ACL imparted 13.4 ± 11.3 N and 12.0 ± 11.6 N more posterior force on the tibia in VL-subluxating knees compared to VL/IR-subluxating knees at 15° and 30° of flexion, respectively ($p \leq 0.030$) (Table 3). Additionally, the ACL imparted 8.6 ± 5.9 N and 7.9 ± 7.0 N more lateral force on the tibia in VL-subluxating knees compared to VL/IR-subluxating knees at 15° and 30° of flexion, respectively ($p \leq 0.030$) (Table 3).

4. Discussion

Our first main finding was that, even though ACL-deficient knees may exhibit the same net motion, their motion patterns might differ markedly. As multiplanar torques were applied to consecutively tested knees, the anterior translation of the lateral tibia followed two distinct motion patterns after the ACL had been sectioned: subluxation with (1) valgus torque alone (VL-subluxating); or with (2) combined valgus and internal rotational torques (VL/IR-subluxating) (Fig. 2). Our second main finding was that these two subgroups of knees are differentiated by their morphology and laxity, and that the ACL, when it was intact, played a different biomechanical role in these two subgroups. Specifically, VL-subluxating knees had higher tibial slope and less anterior laxity with the ACL sectioned than VL/IR-subluxating knees (Tables 1 and 2).

Table 2
Anterior and internal rotational laxities of VL- and VL/IR-subluxating knees with the ACL sectioned.

Laxity Measure and Flexion Angle		VL-subluxating (n = 5)	VL/IR-subluxating (n = 8)	P Value
Anterior Laxity (mm)	15°	–	–	–
	30°	15.7 ± 2.5 (13.5, 17.9)	19.4 ± 1.5 (18.4, 20.5)	0.006
Internal Rotational Laxity (°)	15°	18.6 ± 2.1 (16.8, 20.5)	21.6 ± 2.8 (19.6, 23.5)	0.065
	30°	24.6 ± 3.2 (21.9, 27.4)	27.4 ± 2.2 (25.9, 28.9)	0.171

[1]n = sample size.
[2]The values are given as the mean and standard deviation with the 95% confidence interval in parentheses.

Importantly, at the peak applied valgus torque, the ACL carried more posteriorly- and laterally-directed force when it was intact in VL-subluxating knees (Table 3).

These unique subgroups of knees were unrecognized by previous work that reported only the net tibiofemoral motion (Drews et al., 2017; Engebretsen et al., 2012; Imhauser et al., 2013; Kanamori et al., 2000b, 2002; Lord et al., 2017; Noyes et al., 2017; Rasmussen et al., 2016; Thein et al., 2016; Yamamoto et al., 2006). That said, our observation of distinct motion patterns is corroborated by previous *in vitro* and *in vivo* studies. For example, under pure valgus torque, Kiapour et al. reported variable ACL strain among a set of 19 human cadaveric knees (Kiapour et al., 2015). This parallels our finding of differences in ACL force under pure valgus. Moreover, two independent cases of giving way have been recorded in the gait laboratory in which each subject showed distinct motion patterns (Houck et al., 2003; Houck and Yack, 2001). One subject reported giving way with abnormal abduction and internal rotational moments (Houck and Yack, 2001), while the other reported giving way with only an abnormal abduction moment (Houck et al., 2003).

Surprisingly, we found that the ACL carries increased forces under a broader range of loading conditions (valgus torques alone and combined valgus and internal rotation torques) in VL-subluxating knees. This finding is important because it provides evidence that the ACL serves a more demanding mechanical role in this subgroup. VL-subluxating knees also had increased lateral tibial slope; therefore, our findings may help explain why increased lateral tibial slope is associated with risk of ACL injury (Beynnon et al., 2014). Specifically, in VL-subluxating knees, the ACL must impart a greater, posteriorly- and laterally-directed force on the tibia to resist subluxation of the lateral compartment, which is the pathologic phenomenon generated by pivoting maneuvers (Bedi et al., 2010; Galway and MacIntosh, 1980; Imhauser et al., 2016; Li et al., 2007; Losee, 1983). More frequent mechanical demand on the ACL in VL-subluxating knees may also suggest that these knees are more susceptible to non-contact ACL fatigue failure described by Wojtys et al. (2016).

Table 1
Tibial geometries of VL- and VL/IR-subluxating knees.

Geometric Parameter	VL-subluxating (n = 5)	VL/IR-subluxating (n = 8)	P Value
Sagittal Slope of Lateral Tibial Plateau (°)	2.2 ± 1.7 (0.7, 3.7)	−1.4 ± 1.7 (−2.6, 0.2)	0.003
Sagittal Slope of Medial Tibial Plateau (°)	1.8 ± 1.6 (0.4, 3.2)	2.4 ± 3.2 (0.2, 4.6)	0.833
Anteromedial Tibial Spine Volume (mm^3)	166.2 ± 91.9 (85.7, 246.8)	166.7 ± 85.8 (107.2, 226.1)	0.724

[1]n = sample size.
[2]The values are given as the mean and standard deviation with the 95% confidence interval in parentheses.

Table 3
Component and resultant *In Situ* ACL forces at the peak applied valgus torque (no internal rotation torque) in VL- and VL/IR-subluxating knees.

Force Component and Flexion Angle		VL-subluxating (n = 5)	VL/IR-subluxating (n = 8)	P Value
Proximal ACL Force at Peak Valgus (N)	15°	25.4 ± 11.5 (15.3, 35.4)	12.9 ± 13.9 (3.2, 22.5)	0.127
	30°	20.6 ± 11.6 (10.4, 30.8)	7.4 ± 10.8 (−0.1, 15.0)	0.065
Lateral ACL Force at Peak Valgus (N)	15°	8.2 ± 3.3 (5.3, 11.2)	−0.3 ± 4.9 (−3.7, 3.1)	0.019
	30°	9.2 ± 4.1 (5.6, 12.8)	1.3 ± 5.6 (−2.6, 5.2)	0.030
Posterior ACL Force at Peak Valgus (N)	15°	14.6 ± 9.1 (6.6, 22.5)	1.2 ± 6.7 (−3.5, 5.8)	0.011
	30°	14.9 ± 7.1 (8.6, 21.2)	2.9 ± 9.1 (−3.4, 9.2)	0.030
Resultant ACL Force at Peak Valgus (N)	15°	31.3 ± 12.6 (20.1, 42.3)	15.8 ± 13.0 (6.7, 24.8)	0.093
	30°	27.9 ± 12.1 (17.3, 38.5)	11.4 ± 12.6 (2.7, 20.2)	0.065

[1]n = sample size.
[2]The values are given as the mean and standard deviation with the 95% confidence interval in parentheses.

VL-subluxating knees had greater posterior/inferior-directed slopes on their lateral, and not their medial, tibial plateaus compared to VL/IR-subluxating knees. This corroborates the case-controlled analysis of Beynnon et al. who found that increased lateral, and not medial, slope of the tibia was a risk factor for non-contact ACL-injury (Beynnon et al., 2014). Volume of the medial tibial spine did not differentiate VL- and VL/IR-subluxating knees despite its association with risk of non-contact ACL injury (Sturnick et al., 2014). We speculate that this lack of difference may indicate that the medial tibial spine impacts tibiofemoral motion limits as reported by McDonald et al. rather than the knee's motion pattern (McDonald et al., 2016).

VL-subluxating knees showed less anterior laxity as assessed by a simulated Lachman compared to VL/IR-subluxating knees and a smaller increase in anterior laxity resulting from ACL sectioning (Table 2). Since an ACL-deficient Lachman primarily loads the medial restraints, including the medial meniscus and the medial collateral ligament (Allen et al., 2000; Kanamori et al., 2000a; Papageorgiou et al., 2001), reduced anterior laxity corresponds to a more constrained medial compartment in VL-subluxating knees. Thus, in VL-subluxating knees, the combination of a more constrained medial compartment and a more sloped lateral tibia act to respectively constrain the medial compartment and wedge the lateral compartment anteriorly under pure valgus torque. In contrast, in VL/IR subluxating knees, the flatter lateral tibial slope and more lax medial compartment enables the tibia to remain reduced until the anterior shear force provided by the internal rotation torque drives the lateral compartment anteriorly.

Knowledge of distinct subluxation patterns could also be used to categorize knees during clinical examination by monitoring both the applied loads and the resulting tibial translations. Moreover, clinical implications of these subluxation patterns could be studied by prospectively monitoring clinical outcomes in these two groups. Our finding that the ACL carries increased posterior force in VL-subluxating knees may also have implications for ACL reconstruction (Pietrini et al., 2011; Ziegler et al., 2011). For example, we speculate that lateral, extra-articular augmentation may be indicated in VL-subluxating knees to help resist anterior subluxation, (Sonnery-Cottet et al., 2015). Altogether, our findings may help identify patients in which surgical modifications during ACL reconstruction could mitigate risk of graft failure (Levins et al., 2016). This speculation requires further testing.

This study has limitations. First, the finite resolution of the robot, robot control algorithms, and load cell may impact motion patterns. Even so, the torque convergence tolerance of the robot control algorithms ($\leq$0.4 Nm) was at least 5 times less than the smallest difference in valgus torques at which the lateral compartment subluxated in VL- versus VL/IR-subluxating knees (> 2 Nm); therefore, resolution of the testing system is not a limiting factor. Moreover, groups of VL- and VL/IR-subluxating knees were identical at both 15° and 30° of flexion, further strengthening our finding of unique patterns of motion (Fig. 2). Second is that the precision of the posterior and lateral ACL force components at the peak applied valgus torque was ±0.5 N. Since the smallest, statistically significant difference in ACL force components reported in this study exceeded this error by at least a factor of $\sim$16, this level of uncertainty does not impact our conclusions (Table 3, Appendix I). Third, the applied torques included neither compression comparable to that seen in functional activities (Mundermann et al., 2008; Taylor et al., 2004) nor an additional anterior applied force, which maximizes anterior subluxation of both the medial and lateral compartments (Noyes et al., 2015). Nevertheless, combined valgus and internal rotation torques cause pivoting events, which are the hallmark feature of the ACL-deficient knee (Drews et al., 2017; Engebretsen et al., 2012; Imhauser et al., 2016; Kanamori et al., 2000b, 2002; Lord et al., 2017; Noyes et al., 2015, 2017; Rasmussen et al., 2016; Yamamoto et al., 2006). Fourth, this is a retrospective analysis of a cadaveric biomechanical dataset; to minimize selection bias, specimens were tested consecutively. Further work is needed to evaluate the causality of the relationships presented here, which would require prescreening and grouping of knees prior to testing, systematic changing of variables such as tibial slope via osteotomy, or use of computational modeling (Kia et al., 2016). Fifth, gait involves a varus moment in the stance phase, in which case the medial tibial geometry may play a more important role (Marouane et al., 2015). Thus, future work should evaluate the influence of bony geometry on joint kinematics under additional functional loading scenarios. Finally, motion of the fibular insertion of the LCL has been used in previous studies to track lateral compartment translations, but some use the most lateral border of the tibia plateau, while others use the center of the lateral compartment (Feng et al., 2016; Noyes et al., 2015). However, since lateral compartment translation is the characteristic pathological feature of the ACL-deficient knee in response to rotatory loads applied during the pivot shift exam (Galway and MacIntosh, 1980; Lane et al., 2008a; Losee, 1983) representing motion of the lateral compartment using the fibular insertion of the LCL is adequate.

In conclusion, two subgroups of ACL-sectioned knees exhibited distinct motion patterns in response to multiplanar torques even though their net change in motion did not differ. These patterns were differentiated by risk factors of non-contact ACL injury, namely, sagittal slope of the lateral tibial plateau and the increase in anterior laxity resulting from ACL sectioning (Beynnon et al., 2014; Magnussen et al., 2016). When the ACL was intact, VL-subluxating knees, with their increased lateral tibial slope, subluxated and experienced higher *in situ* ACL force under a broader range of applied loads; thus, in these knees, the ACL may experience greater mechanical demand than in those that subluxated only with combined torques. These findings provide insight into the variable function of the ACL across a subpopulation of knees and the propensity of subgroups of knees to be more susceptible to subluxation events following ACL rupture.

Acknowledgements

This work was funded by the Clark Foundation, the Kirby Foundation, and the Gosnell Family.

Conflict of Interest Statement

The following statement is in reference to the enclosed manuscript entitled "Variations in Anterior Laxity, Sagittal Slope of the Lateral Tibia, and *In Situ* ACL Force Differentiate Knees with Distinct Motion Patterns during a Simulated Pivoting Event." Two of the authors have affiliations with commercial entities not related to this particular study but related to orthopedic surgery. ADP is a consultant for and receives royalties from Zimmer Biomet. TLW receives royalties from Stryker-MAKO Surgical Corporation for designing a patella-femoral prosthesis implant.

Supplementary material

Supplementary data associated with this article can be found, in the online version, at https://doi.org/10.1016/j.jbiomech.2018.04.002.

References

Adams, A.J., Talathi, N.S., Gandhi, J.S., Patel, N.M., Ganley, T.J., 2018. Tibial spine fractures in children: evaluation, management, and future directions. J. Knee Surg.

Allen, C.R., Wong, E.K., Livesay, G.A., Sakane, M., Fu, F.H., Woo, S.L., 2000. Importance of the medial meniscus in the anterior cruciate ligament-deficient knee. J. Orthop. Res. 18, 109–115.

Bedi, A., Musahl, V., Lane, C., Citak, M., Warren, R.F., Pearle, A.D., 2010. Lateral compartment translation predicts the grade of pivot shift: a cadaveric and clinical analysis. Knee Surg. Sports Traumatol. Arthrosc. 18, 1269–1276.

Beynnon, B.D., Hall, J.S., Sturnick, D.R., Desarno, M.J., Gardner-Morse, M., Tourville, T.W., Smith, H.C., Slauterbeck, J.R., Shultz, S.J., Johnson, R.J., Vacek, P.M., 2014. Increased slope of the lateral tibial plateau subchondral bone is associated with greater risk of noncontact ACL injury in females but not in males: a prospective cohort study with a nested, matched case-control analysis. Am. J. Sports Med. 42, 1039–1048.

Burstein, A.H., Wright, T.M., 1994. Fundamentals of Orthopaedic Biomechanics. Williams & Wilkins.

Conteduca, F., Ferretti, A., Mariani, P.P., Puddu, G., Perugia, L., 1991. Chondromalacia and chronic anterior instabilities of the knee. Am. J. Sports Med. 19, 119–123.

Drews, B.H., Kessler, O., Franz, W., Durselen, L., Freutel, M., 2017. Function and strain of the anterolateral ligament part i: Biomechanical analysis. Knee Surg. Sports Traumatol. Arthrosc. 25, 1132–1139.

Engebretsen, L., Wijdicks, C.A., Anderson, C.J., Westerhaus, B., LaPrade, R.F., 2012. Evaluation of a simulated pivot shift test: a biomechanical study. Knee Surg. Sports Traumatol. Arthrosc. 20, 698–702.

Feng, Y., Tsai, T.Y., Li, J.S., Rubash, H.E., Li, G., Freiberg, A., 2016. In-vivo analysis of flexion axes of the knee: femoral condylar motion during dynamic knee flexion. Clin. Biomech. (Bristol, Avon) 32, 102–107.

Fetto, J.F., Marshall, J.L., 1979. Injury to the anterior cruciate ligament producing the pivot-shift sign. J. Bone Joint Surg. Am. 61, 710–714.

Fujie, H., Livesay, G.A., Woo, S.L., Kashiwaguchi, S., Blomstrom, G., 1995. The use of a universal force-moment sensor to determine in-situ forces in ligaments: a new methodology. J. Biomech. Eng. 117, 1–7.

Galway, H.R., MacIntosh, D.L., 1980. The lateral pivot shift: a symptom and sign of anterior cruciate ligament insufficiency. Clin. Orthop. Relat. Res., 45–50

Grood, E.S., Suntay, W.J., 1983. A joint coordinate system for the clinical description of three-dimensional motions: application to the knee. J. Biomech. Eng. 105, 136–144.

Houck, J., Lerner, A., Gushue, D., Yack, H.J., 2003. Self-reported giving-way episode during a stepping-down task: Case report of a subject with an ACL-deficient knee. J. Orthop. Sports Phys. Ther. 33, 273–282; discussion 283–276.

Houck, J., Yack, H.J., 2001. Giving way event during a combined stepping and crossover cutting task in an individual with anterior cruciate ligament deficiency. J. Orthop. Sports Phys. Ther. 31, 481–489; discusssion 490–485.

Imhauser, C., Mauro, C., Choi, D., Rosenberg, E., Mathew, S., Nguyen, J., Ma, Y., Wickiewicz, T., 2013. Abnormal tibiofemoral contact stress and its association with altered kinematics after center-center anterior cruciate ligament reconstruction: an in vitro study. Am. J. Sports Med. 41, 815–825.

Imhauser, C.W., Sheikh, S., Choi, D.S., Nguyen, J.T., Mauro, C.S., Wickiewicz, T.L., 2016. Novel measure of articular instability based on contact stress confirms that the anterior cruciate ligament is a critical stabilizer of the lateral compartment. J. Orthop. Res. 34, 478–488.

Jonsson, H., Riklund-Ahlstrom, K., Lind, J., 2004. Positive pivot shift after ACL reconstruction predicts later osteoarthrosis: 63 patients followed 5–9 years after surgery. Acta Orthop. Scand. 75, 594–599.

Kanamori, A., Sakane, M., Zeminski, J., Rudy, T.W., Woo, S.L., 2000a. In-situ force in the medial and lateral structures of intact and ACL-deficient knees. J. Orthop. Sci. 5, 567–571.

Kanamori, A., Woo, S.L., Ma, C.B., Zeminski, J., Rudy, T.W., Li, G., Livesay, G.A., 2000b. The forces in the anterior cruciate ligament and knee kinematics during a simulated pivot shift test: a human cadaveric study using robotic technology. Arthroscopy 16, 633–639.

Kanamori, A., Zeminski, J., Rudy, T.W., Li, G., Fu, F.H., Woo, S.L., 2002. The effect of axial tibial torque on the function of the anterior cruciate ligament: a biomechanical study of a simulated pivot shift test. Arthroscopy 18, 394–398.

Kaufman, L., Rousseeuw, P.J., 1987. Clustering by means of medoids. In: Dodge, Y. (Ed.), Statistical data analysis based on the l1-norm and related methods. Birkhäuser Basel, Switzerland, pp. 405–416.

Kawasaki Robotics, 1999. C series controller, operations, and programming manual. Kawasaki Robotics, Training and Documentation Department, Wixom, Michigan.

Kia, M., Schafer, K., Lipman, J., Cross, M., Mayman, D., Pearle, A., Wickiewicz, T., Imhauser, C., 2016. A multibody knee model corroborates subject-specific experimental measurements of low ligament forces and kinematic coupling during passive flexion. J. Biomech. Eng. 138, 051010.

Kiapour, A.M., Kiapour, A., Goel, V.K., Quatman, C.E., Wordeman, S.C., Hewett, T.E., Demetropoulos, C.K., 2015. Uni-directional coupling between tibiofemoral frontal and axial plane rotation supports valgus collapse mechanism of ACL injury. J. Biomech. 48, 1745–1751.

Kocher, M.S., Steadman, J.R., Briggs, K.K., Sterett, W.I., Hawkins, R.J., 2004. Relationships between objective assessment of ligament stability and subjective assessment of symptoms and function after anterior cruciate ligament reconstruction. Am. J. Sports Med. 32, 629–634.

Lane, C.G., Warren, R., Pearle, A.D., 2008a. The pivot shift. J. Am. Acad. Orthop. Surg. 16, 679–688.

Lane, C.G., Warren, R.F., Stanford, F.C., Kendoff, D., Pearle, A.D., 2008b. In vivo analysis of the pivot shift phenomenon during computer navigated ACL reconstruction. KneeSurg Sports Traumatol. Arthrosc. 16, 487–492.

Leitze, Z., Losee, R.E., Jokl, P., Johnson, T.R., Feagin, J.A., 2005. Implications of the pivot shift in the ACL-deficient knee. Clin. Orthop. Relat. Res., 229–236

Levins, J.G., Sturnick, D.R., Argentieri, E.C., Gardner-Morse, M., Vacek, P.M., Desarno, M.J., Tourville, T.W., Slauterbeck, J.R., Beynnon, B.D., 2016. Geometric risk factors associated with noncontact anterior cruciate ligament graft rupture. Am. J. Sports Med. 44, 2537–2545.

Li, G., Papannagari, R., DeFrate, L.E., Yoo, J.D., Park, S.E., Gill, T.J., 2007. The effects of ACL deficiency on mediolateral translation and varus-valgus rotation. Acta Orthop. 78, 355–360.

Lord, B.R., El-Daou, H., Sabnis, B.M., Gupte, C.M., Wilson, A.M., Amis, A.A., 2017. Biomechanical comparison of graft structures in anterior cruciate ligament reconstruction. Knee Surg. Sports Traumatol. Arthrosc. 25, 559–568.

Losee, R.E., 1983. Concepts of the pivot shift. Clin. Orthop. Relat. Res., 45–51

Magnussen, R.A., Reinke, E.K., Huston, L.J., Group, M., Hewett, T.E., Spindler, K.P., 2016. Effect of high-grade preoperative knee laxity on anterior cruciate ligament reconstruction outcomes. Am. J. Sports Med. 44, 3077–3082.

Marouane, H., Shirazi-Adl, A., Hashemi, J., 2015. Quantification of the role of tibial posterior slope in knee joint mechanics and ACL force in simulated gait. J. Biomech. 48, 1899–1905.

McCarthy, M.M., Tucker, S., Nguyen, J.T., Green, D.W., Imhauser, C.W., Cordasco, F.A., 2013. Contact stress and kinematic analysis of all-epiphyseal and over-the-top pediatric reconstruction techniques for the anterior cruciate ligament. Am. J. Sports Med. 41, 1330–1339.

McDonald, L.S., Boorman-Padgett, J., Kent, R., Stone, K., Wickiewicz, T.L., Pearle, A.D., Imhauser, C.W., 2016. Acl deficiency increases forces on the medial femoral condyle and the lateral meniscus with applied rotatory loads. J. Bone Joint Surg. Am. 98, 1713–1721.

Mundermann, A., Dyrby, C.O., D'Lima, D.D., Colwell Jr., C.W., Andriacchi, T.P., 2008. In vivo knee loading characteristics during activities of daily living as measured by an instrumented total knee replacement. J. Orthop. Res. 26, 1167–1172.

Noyes, F.R., Huser, L.E., Levy, M.S., 2017. Rotational knee instability in ACL-deficient knees: Role of the anterolateral ligament and iliotibial band as defined by tibiofemoral compartment translations and rotations. J. Bone Joint Surg. Am. 99, 305–314.

Noyes, F.R., Jetter, A.W., Grood, E.S., Harms, S.P., Gardner, E.J., Levy, M.S., 2015. Anterior cruciate ligament function in providing rotational stability assessed by medial and lateral tibiofemoral compartment translations and subluxations. Am. J. Sports Med. 43, 683–692.

Noyes, F.R., McGinniss, G.H., Grood, E.S., 1985. The variable functional disability of the anterior cruciate ligament-deficient knee. Orthop. Clin. North. Am. 16, 47–67.

Papageorgiou, C.D., Gil, J.E., Kanamori, A., Fenwick, J.A., Woo, S.L., Fu, F.H., 2001. The biomechanical interdependence between the anterior cruciate ligament replacement graft and the medial meniscus. Am. J. Sports Med. 29, 226–231.

Pietrini, S.D., Ziegler, C.G., Anderson, C.J., Wijdicks, C.A., Westerhaus, B.D., Johansen, S., Engebretsen, L., LaPrade, R.F., 2011. Radiographic landmarks for tunnel positioning in double-bundle ACL reconstructions. Knee Surg. Sports Traumatol. Arthrosc. 19, 792–800.

Prisk, V.R., Imhauser, C.W., O'Loughlin, P.F., Kennedy, J.G., 2010. Lateral ligament repair and reconstruction restore neither contact mechanics of the ankle joint nor motion patterns of the hindfoot. J. Bone Joint Surg. Am. 92, 2375–2386.

Rasmussen, M.T., Nitri, M., Williams, B.T., Moulton, S.G., Cruz, R.S., Dornan, G.J., Goldsmith, M.T., LaPrade, R.F., 2016. An in vitro robotic assessment of the anterolateral ligament, part 1: Secondary role of the anterolateral ligament in the setting of an anterior cruciate ligament injury. Am. J. Sports Med. 44, 585–592.

Schon, J.M., Moatshe, G., Brady, A.W., Serra Cruz, R., Chahla, J., Dornan, G.J., Turnbull, T.L., Engebretsen, L., LaPrade, R.F., 2016. Anatomic anterolateral ligament reconstruction of the knee leads to overconstraint at any fixation angle. Am. J. Sports Med. 44, 2546–2556.

Sonnery-Cottet, B., Thaunat, M., Freychet, B., Pupim, B.H., Murphy, C.G., Claes, S., 2015. Outcome of a combined anterior cruciate ligament and anterolateral ligament reconstruction technique with a minimum 2-year follow-up. Am. J. Sports Med. 43, 1598–1605.

Sturnick, D.R., Argentieri, E.C., Vacek, P.M., DeSarno, M.J., Gardner-Morse, M.G., Tourville, T.W., Slauterbeck, J.R., Johnson, R.J., Shultz, S.J., Beynnon, B.D., 2014. A decreased volume of the medial tibial spine is associated with an increased risk of suffering an anterior cruciate ligament injury for males but not females. J. Orthop. Res. 32, 1451–1457.

Tamea Jr., C.D., Henning, C.E., 1981. Pathomechanics of the pivot shift maneuver. an instant center analysis. Am. J. Sports Med. 9, 31–37.

Taylor, W.R., Heller, M.O., Bergmann, G., Duda, G.N., 2004. Tibio-femoral loading during human gait and stair climbing. J. Orthop. Res. 22, 625–632.

Thein, R., Boorman-Padgett, J., Stone, K., Wickiewicz, T.L., Imhauser, C.W., Pearle, A. D., 2016. Biomechanical assessment of the anterolateral ligament of the knee: a secondary restraint in simulated tests of the pivot shift and of anterior stability. J. Bone Joint Surg. Am. 98, 937–943.

Tochigi, Y., Vaseenon, T., Heiner, A.D., Fredericks, D.C., Martin, J.A., Rudert, M.J., Hillis, S.L., Brown, T.D., McKinley, T.O., 2011. Instability dependency of osteoarthritis development in a rabbit model of graded anterior cruciate ligament transection. J. Bone Joint Surg. Am. 93, 640–647.

Uhorchak, J.M., Scoville, C.R., Williams, G.N., Arciero, R.A., St Pierre, P., Taylor, D.C., 2003. Risk factors associated with noncontact injury of the anterior cruciate ligament: a prospective four-year evaluation of 859 west point cadets. Am. J. Sports Med. 31, 831–842.

Vacek, P.M., Slauterbeck, J.R., Tourville, T.W., Sturnick, D.R., Holterman, L.A., Smith, H.C., Shultz, S.J., Johnson, R.J., Tourville, K.J., Beynnon, B.D., 2016. Multivariate analysis of the risk factors for first-time noncontact ACL injury in high school and college athletes: a prospective cohort study with a nested, matched case-control analysis. Am. J. Sports Med. 44, 1492–1501.

van Eck, C.F., van den Bekerom, M.P., Fu, F.H., Poolman, R.W., Kerkhoffs, G.M., 2013. Methods to diagnose acute anterior cruciate ligament rupture: a meta-analysis of physical examinations with and without anaesthesia. Knee Surg. Sports Traumatol. Arthrosc. 21, 1895–1903.

Viidik, A., 1973. Functional properties of collagenous tissues. Int. Rev. Connect. Tissue Res. 6, 127–215.

Wojtys, E.M., Beaulieu, M.L., Ashton-Miller, J.A., 2016. New perspectives on ACL injury: on the role of repetitive sub-maximal knee loading in causing ACL fatigue failure. J. Orthop. Res. 34, 2059–2068.

Woo, S.L., Fox, R.J., Sakane, M., Livesay, G.A., Rudy, T.W., Fu, F.H., 1998. Biomechanics of the ACL: measurements of in situ force in the ACL and knee kinematics. Knee 5, 267–288.

Yamamoto, Y., Hsu, W.H., Fisk, J.A., Van Scyoc, A.H., Miura, K., Woo, S.L., 2006. Effect of the iliotibial band on knee biomechanics during a simulated pivot shift test. J. Orthop. Res. 24, 967–973.

Ziegler, C.G., Pietrini, S.D., Westerhaus, B.D., Anderson, C.J., Wijdicks, C.A., Johansen, S., Engebretsen, L., LaPrade, R.F., 2011. Arthroscopically pertinent landmarks for tunnel positioning in single-bundle and double-bundle anterior cruciate ligament reconstructions. Am. J. Sports Med. 39, 743–752.